

Laser-Induced Breakdown Spectroscopy

A Senior Project

presented to

the Faculty of the Physics Department

California Polytechnic State University, San Luis Obispo

In Partial Fulfillment

of the Requirements for the Degree

Bachelor of Science in Physics

by

Connor Drake

June, 2011

© 2011 Connor Drake

Table of Contents

Abstract and Research Goals 3

Introduction and Basic Theories 3

Energy Level Theory (Bohr Model) 7

Experimental Setup and Procedure 7

Laser Output 10

Electronic Timeline Leading to Laser Fire 11

Data and Data Analysis 11

Applications: Spectroscopy of Solids 17

Conclusions 20

Poster 20

References 21

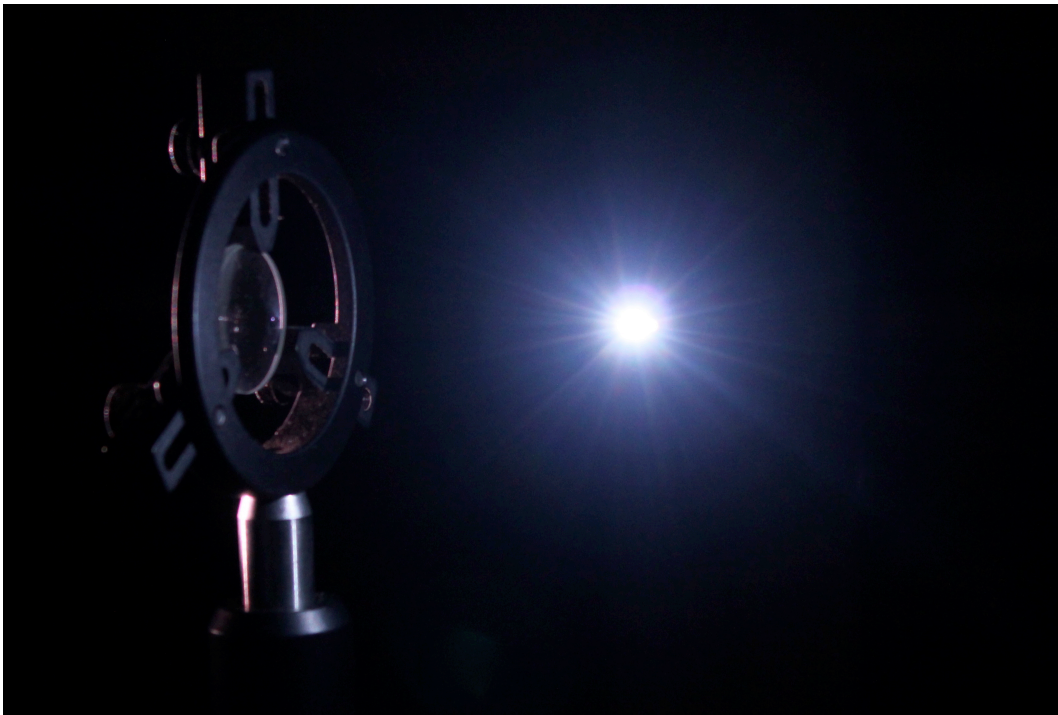


Figure 1: Plasma spark and focusing lens

Abstract and Research Goals

The goal of this work is to use a Neodymium-Doped Yttrium Aluminum Garnet (Nd:YAG) Laser, spectrometer, and computer to create a Laser Induced Breakdown Spectroscopy (LIBS) system. LIBS utilizes a focused, high-powered, pulsed laser whose peak electric field ionizes materials at the beam focal point, creating localized plasma. The plasma state includes broken molecular bonds, atom/electron-ionization, and excited electrons, which on the macroscopic level is a loud “snap” and a bright spark. In this project, a fiber optic cable is used to capture light emitted from the spark, and direct it into a spectrometer which tallies the number of photons at each wavelength, resulting in a characteristic spectrum of the light produced. Because each photon corresponds to a specific energy transition within the plasma, the spectrum can be used to determine the composition of the material and relative abundance of elements. With careful equipment synchronization, we were able to assemble and test a working computer-controlled LIBS system. Data is presented for various samples including the atmosphere and metallic coin surfaces.

Introduction and Basic Theories

The central physical principal is the formation of the plasma spark from the sample using the laser output. Plasma is a fourth state of matter that is formed when a gaseous sample is heated to the point that the molecular bonds within the sample are broken, resulting in ions of the sample’s basic atoms. The deionization of the plasma and the return of the excited electrons return to their ground level state produces photons, with each photon energy corresponding to the energy difference between the excited and ground states. This is the physical process that produces the visible spark observed within the lab. Using the Planck-Einstein relation, shown below, it can be seen that each of the specific photon energies correspond to a unique wavelength that can be measured in lab using a spectrometer.

$$E = \frac{hc}{\lambda}$$

There is potentially some further very high-level theory involved in this experiment regarding the formation and dissolution of the plasma created at the laser focal point, however I plan on focusing more on the theoretical elements of the laser itself.

The intensity I of a laser is defined as the ratio of power output P to the cross sectional area A of the output, resulting in the equation below.

$$I = \frac{P}{A}$$

This implies that an increase in power output or a decrease in the cross-sectional area. A LIBS laser system achieves such a great intensity by having an extremely high power output, which is further focused into a smaller area. The electromagnetic radiation of the laser output creates an electric field. Once the intensity of the laser at the focal point is known, the magnitude of the electric field $|\vec{E}|$ created at the focal point can be calculated using the equation below.

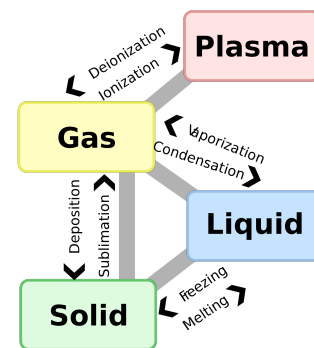


Figure 2: Plasma as a fourth state of matter

$$I = \frac{1}{2} c^2 \epsilon_0^2 |\bar{E}|^2 \quad \text{which rearranges to} \quad |\bar{E}| = \sqrt{\frac{2(I)}{c \epsilon_0}}$$

The duty cycle D of a periodic event, such as a pulsed laser fire, is determined by the ratio of the time spent “active” τ to the entire period T . Using a photodiode and oscilloscope we verified that the laser was pulsing at 10Hz for a duration of 4.3ns to each pulse. Converting frequency to period and taking the ratio of “active” time to total period, the duty cycle for our laser can be calculated.

$$D = \frac{\tau}{T} = \frac{4.3 \times 10^{-9} s}{0.1 s} = 4.3 \times 10^{-6} \%$$

This means that the laser spends 99.999995% of the time off and outputting no power, which explains the measured average power output of only 4W. Using the definition of power,

$$P_{average} = \frac{E_{pulse}}{t_{total}}$$

we can find the total energy output per pulse.

$$E_{pulse} = (P_{average})(t) = (4W)(0.1s) = 400mJ$$

Recalculating the power output during the laser fire,

$$P_{pulse} = \frac{E_{pulse}}{t_{pulse}} = \frac{400mJ}{4.3 \times 10^{-9} s} = 93.0MW$$

yields an incredibly high power output. Since we can also measure the beam diameter at both the laser output and the focal points, we can use this power to calculate the intensity at electric field when the laser is firing.

We measured the laser output to be a beam with a diameter of 1mm, which is then focused down to approximately a 0.2mm focal point. However, the focal point could be smaller than 0.2mm in reality because it was difficult to accurately measure such a small burn mark. Also the central intensity of the beam was smaller than the total burn area because the intensity is not perfectly constant throughout the entire beam. The image below is of actual laser burn patterns used to measure the beam diameter, though they are much magnified.

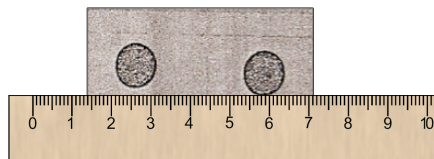


Figure 3: Laser burn marks at 30cm unfocused (mm units)

The diagram below illustrates the geometry of the laser output and how the lens decreases the cross-sectional area of the beam by almost an order of magnitude.

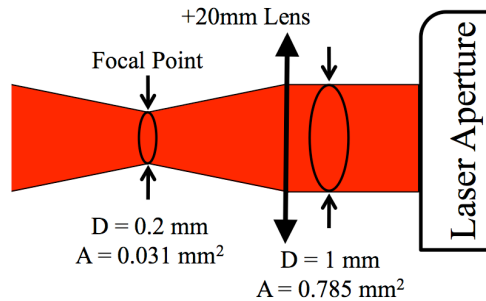


Figure 4: Laser output profile with measured beam area

Using the previous definition of intensity and calculated cross-sectional areas of the beam at each point:

$$I_{unfocused} = \frac{P_{pulse}}{A_{unfocused}} = \frac{93.0 MW}{\pi(0.5 mm)^2} = 1.185 \times 10^{14} W / m^2 \approx 119 TW / m^2$$

$$I_{focused} = \frac{P_{pulse}}{A_{focused}} = \frac{93.0 MW}{\pi(0.1 mm)^2} = 2.961 \times 10^{15} W / m^2 \approx 2960 TW / m^2$$

Using the previous formula relating electric field magnitude to intensity via c , the speed of light in a vacuum, and ϵ_0 , the electric constant, we can calculate the corresponding electric fields within the focused and unfocused beam.

$$|\bar{E}_{unfocused}| = \sqrt{\frac{2(I_{unfocused})}{c\epsilon_0}} = \sqrt{\frac{2(1.185 \times 10^{14} W / m^2)}{(3 \times 10^8 m / s)(8.9 \times 10^{-12} C / Vm)}} = 2.987 \times 10^8 V / m \approx 0.298 GV / m$$

$$|\bar{E}_{focused}| = \sqrt{\frac{2(I_{focused})}{c\epsilon_0}} = \sqrt{\frac{2(2.961 \times 10^{15} W / m^2)}{(3 \times 10^8 m / s)(8.9 \times 10^{-12} C / Vm)}} = 1.49 \times 10^9 V / m \approx 1.5 GV / m$$

These calculated values of YAG intensity and electric field are somewhat abstract, so for comparison we calculated the same values for a typical, unfocused red HeNe laser. Such a laser might output a constant 0.1mW in a 3mm beam and have the following intensity and electric field:

$$I_{HeNe} = \frac{P_{HeNe}}{A_{HeNe}} = \frac{0.1 mW}{\pi(1.5 mm)^2} = 14.1 W / m^2$$

$$|\bar{E}_{HeNe}| = \sqrt{\frac{2(I_{HeNe})}{c\epsilon_0}} = \sqrt{\frac{2(14.1 W / m^2)}{(3 \times 10^8 m / s)(8.9 \times 10^{-12} C / Vm)}} = 103 V / m$$

To put these numbers in perspective, the YAG laser is one hundred quadrillion times as intense at its focal point than a hypothetical typical HeNe laser pointer.

These values can also be compared to an estimate of the laser intensity and electric field at the National Ignition Facility (NIF) at Lawrence Livermore National Laboratory (LLNL). The laboratory website reports that each of the 192 laser pulses carry 20kJ of energy, and all lasers are focused onto a target pellet several millimeters in diameter. All laser pulses last on the order of a nanosecond and reach the target pellet simultaneously within 30 picoseconds accuracy. Making some rough estimates of the beam timing and the surface area of the target pellet, we can calculate the intensity and electric field of NIF for comparison.

$$I_{NIF} = \frac{E_{NIF}}{t_{NIF} A_{NIF}} = \frac{\left(20 \frac{kJ}{pulse}\right)(192 pulse)}{(1ns) \left(4\pi \left(\frac{3mm}{2}\right)^2\right)} = 1.36 \times 10^{20} W / m^2 \approx 136 EW / m^2$$

$$|\vec{E}_{NIF}| = \sqrt{\frac{2(I_{NIF})}{c \epsilon_0}} = \sqrt{\frac{2(1.36 \times 10^{20} W / m^2)}{(3 \times 10^8 m / s)(8.9 \times 10^{-12} C / Vm)}} = 3.20 \times 10^{11} V / m \approx 319 GV / m$$

Comparing the YAG to the NIF rather than a common laser pointer, we see that NIF is about 50,000 times more intense than our YAG and generates an electric field with about 250 times greater of a magnitude.

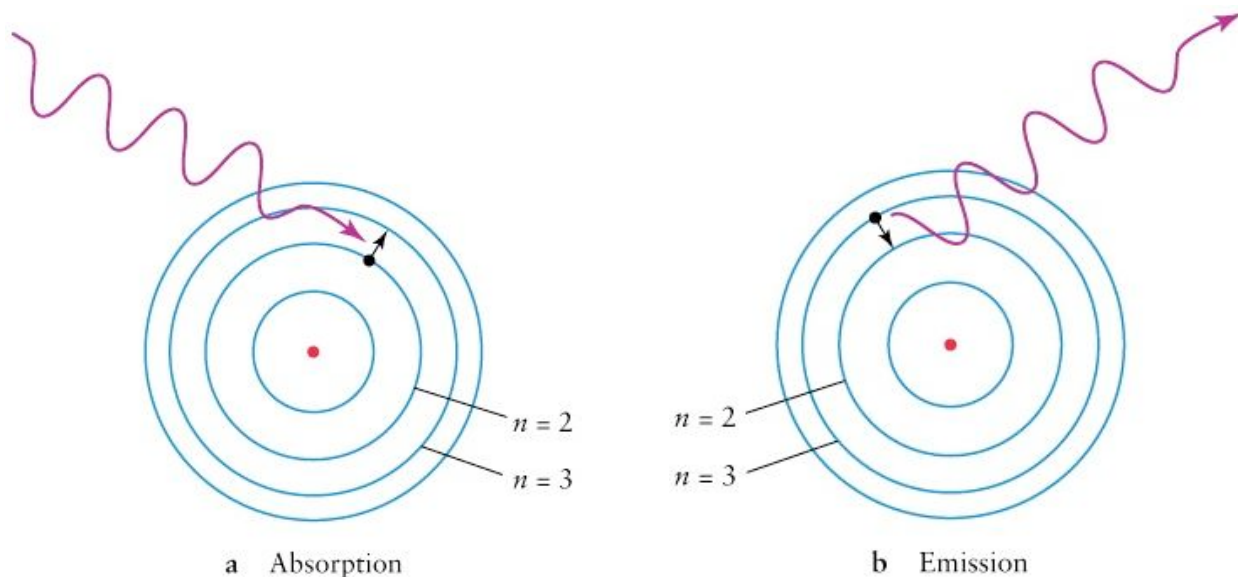
Energy Level Theory (Bohr Model)

As mentioned previously, the plasma formed from various materials will emit a spectrum of photons with a unique combination of energy levels when the excited electrons return to their ground states during the deionization of the plasma. Though the exact process of absorption/emission of photons in the formation and deionization of plasma is much more complicated, the Bohr model of the hydrogen atom can be used to nicely illustrate the process the electron goes through at an atomic level.

The Bohr model describes a hydrogen atom as a small, dense, positively charged nucleus, surrounded by a small, negatively charged electron moving around the nucleus with a circular orbit. This model was created to describe only the hydrogen atom, but can be used to roughly model larger atoms with a greater quantity of protons and electrons.

Niels Bohr, the creator of the model, hypothesized that the electrons orbit classically around the nucleus and only at a discrete set of distances. He called this discrete set of allowed orbits the ‘energy shells’ of the atom, where each shell is associated with an exact energy. If an electron in a lower energy shell is hit by an incident photon, whose energy is equal to the energy difference between the lower energy shell and some higher energy shell, the electron will ‘jump’ up to the excited state. This is illustrated in diagram (a) below, where the incident photon is absorbed and the electron jumps from the n=2 to the n=3 state. After some time, the electron de-excites and

returns to its pre-excited ground state, emitting a photon corresponding to the energy difference between the states. This is illustrated in diagram (b) below.



This combination of photon absorption/emission occurs in LIBS when the photons from the laser ionize the sample and excite the electrons. After the average lifetime of the excited energy state, the electrons de-excite by photon emission, creating the visible spark, which is measured in the lab. Since the photon energies, or wavelengths, depend on the energy differences, which differ in every atom, the spectrum of photons emitted will create a unique fingerprint for each element.

Experimental Setup and Procedure

For future reference, we have compiled an exhaustive list of step-by-step instructions to reproduce this LIBS setup.

1. Put on safety glasses corresponding to the lasing wavelength desired. Depending on the additional crystal, the laser can output 1064nm or 532nm. Also verify that beam dump and other protective steps are taken.
2. Power on YAG laser using key. Open shutter on laser and use control pad to begin laser fire. Verify that system can run in the automatic setting, firing at 10Hz.
3. Place a short focal length lens along the beam path such that a plasma spark is created at the focal point. Turn up laser intensity until spark is formed.
4. Connect fiber optic cable with lens to spectrometer. Place lens several inches from laser spark, aligned as precisely as possible. This can be further adjusted laser to optimize the intensity of the collected light.
5. With laser fire stopped, connect spectrometer to computer using USB cable and open LIBS software on computer.
6. Connect spectrometer to laser system using custom cable with three outputs to laser: Lamp In, Lamp Out, and Q-switch. The Lamp In cable connects to the Input Flashlamp Synchronization, the Lamp Out cable connects to the Output Flashlamp Synchronization, and the Q-switch cable connects to the Input Q-switch Synchronization.

7. Push buttons on the front panel of the laser to set the Flashlamp and Q-switch in external mode. The EXT lights should light up red when properly set.
8. Use LIBS software to set number of shots to fire and how many bursts to average. The Q-switch delay can also be set internally in the software*.
9. Click FIRE within the software. The laser should fire, creating a spark and displaying the collected spectrum of the atmosphere on-screen. This spectrum image can be saved or exported to a spreadsheet for further analysis.
10. To collect other solid samples, place the surface of the sample at the focal point of the laser beam. The spark will ionize the sample, along with the atmosphere and display the collected spectra. To isolate the sample spectra, the subtract background feature of the software can be used.
11. *The Q-switch can also more accurately be set using a delay box attached between the Q-switch output of the spectrometer and the Input Q-switch Synchronization. In this case, the software Q-switch delay is set to zero and all adjustments are made manually using the delay box.

The diagram below shows the layout and connections between the various components of the created LIBS setup. The individual components and description of the connections between each component are also described in further detail below the diagram.

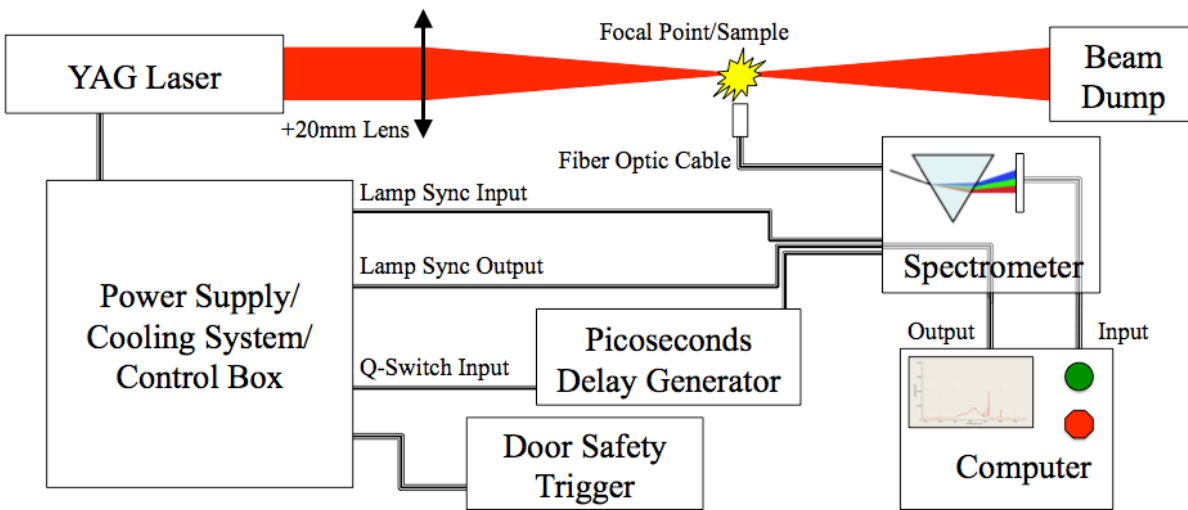


Figure 5: LIBS system experimental setup

The Quantel YAG Laser diagram from the operator manual is shown below. Element (1) is the electronics receiving the Q-switch command for the laser to fire, and elements (2) - (9) are the central components in the lasing process. The rest of the elements are related to the laser housing and adjustments for the focus and alignment.

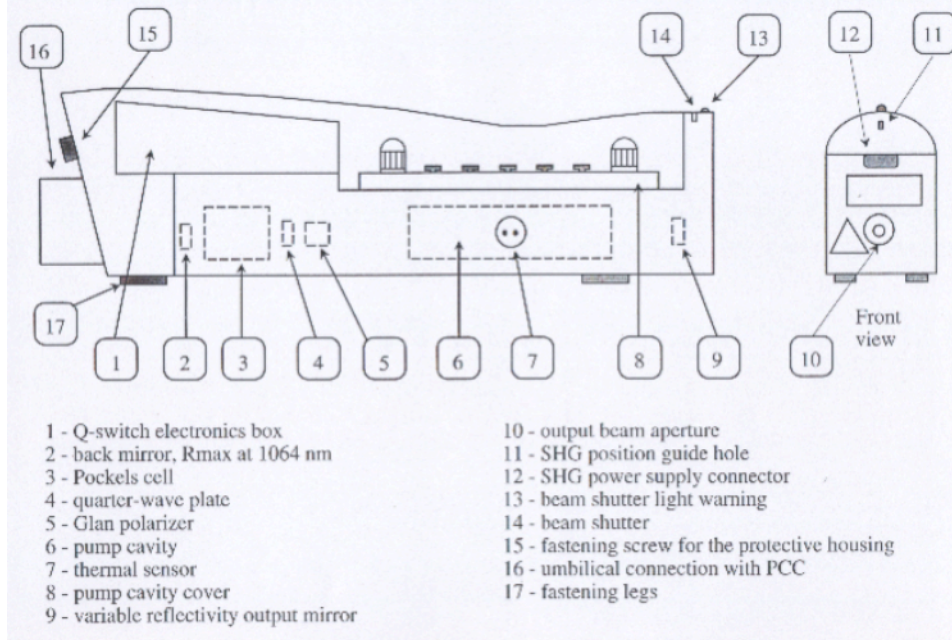


Figure 6: Laser housing diagram

The laser is then connected to a housing for the: power supply, cooling system, laser control circuitry, and capacitors, which store the energy dumped into the laser. The internal components of this control box are shown below.

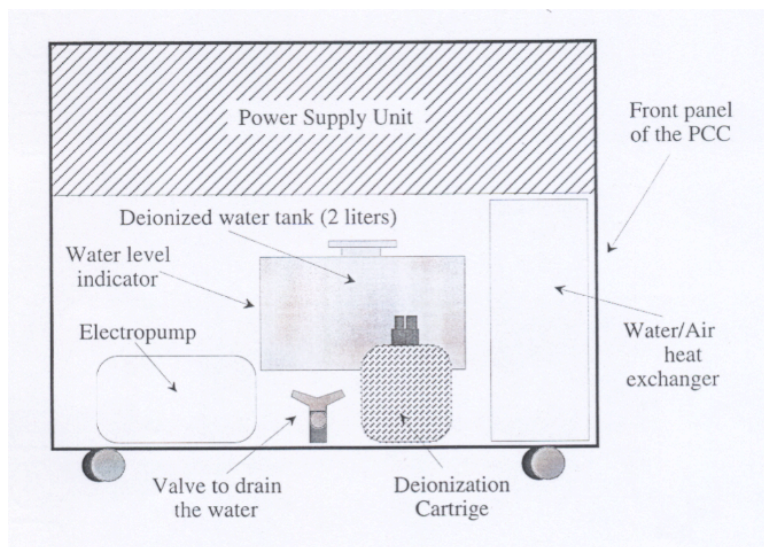


Figure 7: Laser control box diagram

The laser output is focused through a 20mm converging lens, creating a focal point with a strong enough electric field to ionize the material present into localized plasma. The laser beam is then directed into a beam dump to minimize reflected radiation. The light created by the plasma is collected by a small lens and focused into a fiber optic cable connected to an Ocean Optics HR2000 Spectrometer. The spectrometer splits the collected light by wavelength and counts the photons at each wavelength. This data is sent to a connected computer, which uses Ocean Optics

LIBS software to display the collected spectrum. The computer software is also used to control the firing and timing of the system. The computer communicates with the laser control via the spectrometer, which connects three cables to the laser control: lamp sync input, lamp sync output, and q-switch input, which is sent through a delay generator box that is accurate down to the pico-second. Lastly, the laser control box is connected to an interlock safety system linked to the door of the lab so that if the door is opened while the laser is operating, the system shuts down.

Laser Output

The YAG laser light is in the infrared range of the electromagnetic spectrum at 1064 nm. As mentioned previously, the pulses are 4.3ns at 10Hz, with each pulse containing 400 mJ of energy. Since we know the wavelength of the laser light, we can use Planck's relation to calculate the energy per photon in the laser beam.

$$E_{\text{photon}} = \frac{hc}{\lambda} = \frac{1240\text{nm}}{1064\text{nm}} = 1.165\text{eV}$$

If each photon carries 1.165eV of energy and we know the total energy contained within each pulse, we can solve for the mean number of photons emitted over the duration of each pulse.

$$N_{\text{photons}} = \frac{E_{\text{pulse}}}{E_{\text{photon}}} = \frac{400\text{mJ}}{1.165\text{eV}} \frac{1\text{eV}}{1.602 \times 10^{-16}\text{mJ}} = 2.14 \times 10^{18}$$

The diagram below is of the power output of the laser over time. Though not to scale, it nicely illustrates the laser's short duty cycle and difference between average power output and power output during a pulse.

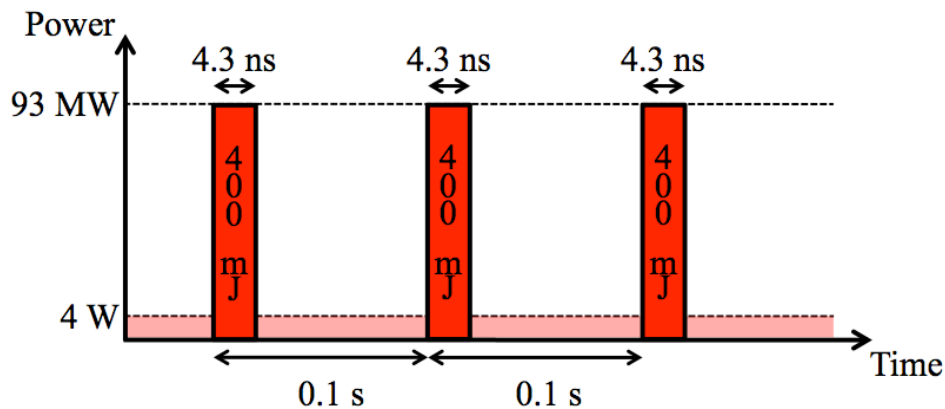


Figure 8: Duty cycle timing with max and average power outputs

The laser cross section is measured using data from the last quality control test data. Part of this data is a visual laser output cross section of the intensity with measurements of the major and minor widths. This intensity cross section is shown below. The output is very nearly circular with a slight variance in intensity radiating outwards from the beam center.

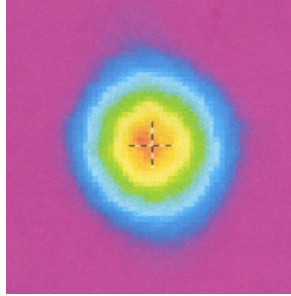


Figure 9: Intensity cross section of laser beam

Electronic Timeline Leading to Laser Fire

The first step in the setup of the LIBS system was to analyze the electronic signals sent between the various components to determine the correct connections and timing settings. This was done using an oscilloscope connected into the various component input and outputs as well as a photodiode to analyze the timing of the laser fire itself.

The first signal that occurs after clicking in the software is the lamp synchronization input pulse (Lamp Sync In), which is sent from the computer to the laser control via the spectrometer. The Lamp Sync In tells the laser to get ready to fire by charging its capacitors. Once the laser has charged its capacitors, it sends a lamp synchronization output pulse (Lamp Sync Out) back to the computer to say it is ready to fire. After a delay time set in the computer software, the computer sends a q-switch input (Q-Switch In) back to the laser, telling it to fire. The laser quickly discharges its capacitors and fires within the duration of the Q-Switch In pulse. The timing diagram of these four events is shown below.

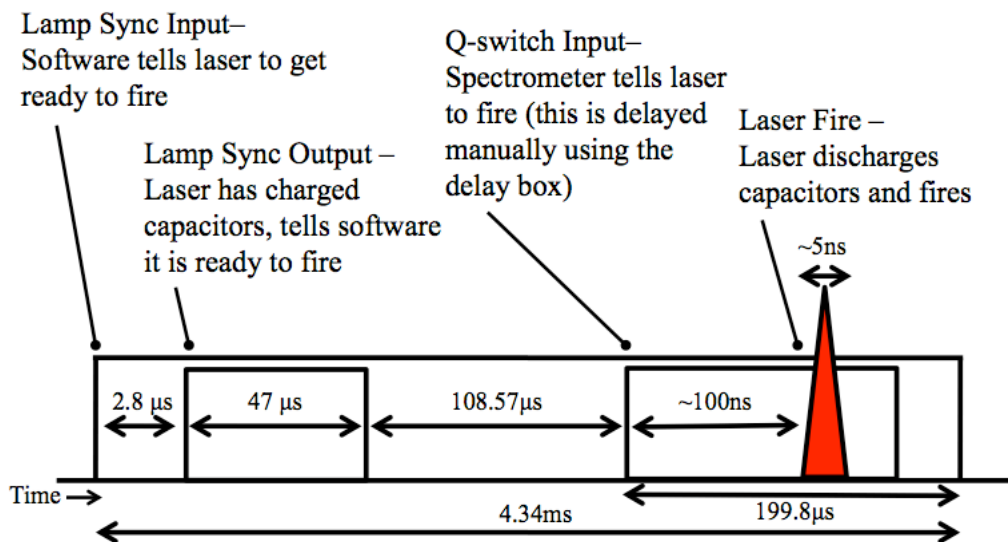
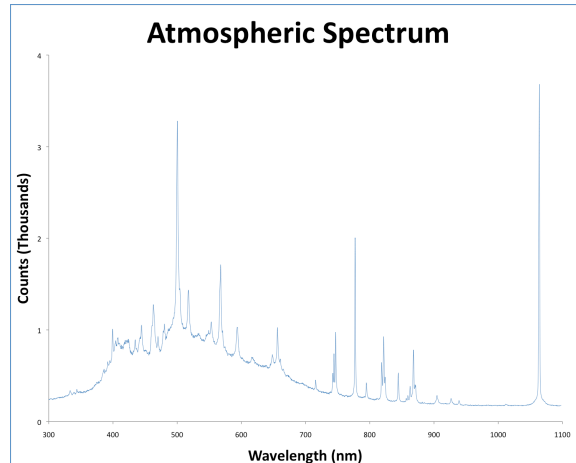


Figure 10: Laser fire electronic signals diagram

Data and Data Analysis

All data collected in this experiment was of counts vs. wavelength for each sample tested. When plotted, this produced a spectrum of the light produced by the plasma.

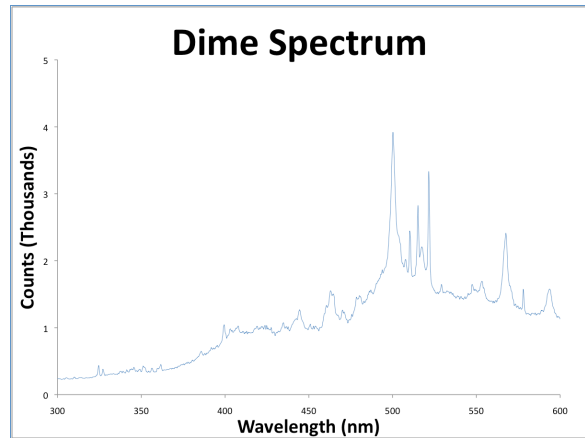
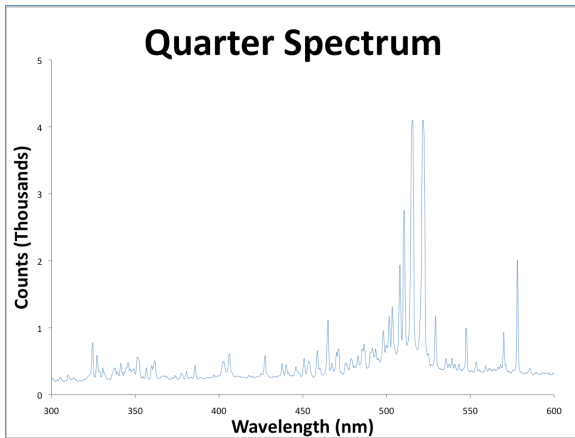
The first spectrum collected, to verify the system was working correctly and hold as a standard for comparison to other spectra, was simply the atmospheric spectrum. This was accomplished by allowing the laser to simply ionize the nitrogen and oxygen in the air in the laboratory. This is the collected spectrum for the atmosphere.



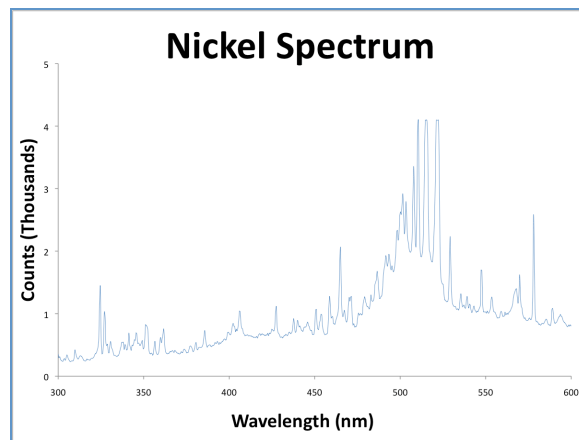
The large peak at the right side at 1064nm is the laser output. Ideally the timing of the system could be adjusted so that the laser output was not detected when the spectrometer samples the plasma spark, however we were unable to adjust the timing properly. Apart from the laser output peak, there are many other distinct peaks, mostly in the 400nm to 900nm range that we will assert are from the excited electrons de-exciting. Once used to verify the system was working properly, the atmospheric spectra was saved in the spectrometer software as the background reading, which allowed us to subtract off the atmospheric spectrum from the collected sample spectra. This would theoretically yield a spectrum with little or no noise, though in practice the variance in the relative intensities of the light collected from the plasma deionization resulted in the technique not being able to perfectly cancel out the background.

The first solid samples taken were of US coin currency. Coins were selected because they are of a known mixture of metals and multiples of the same coin could be compared to verify the system was working correctly.

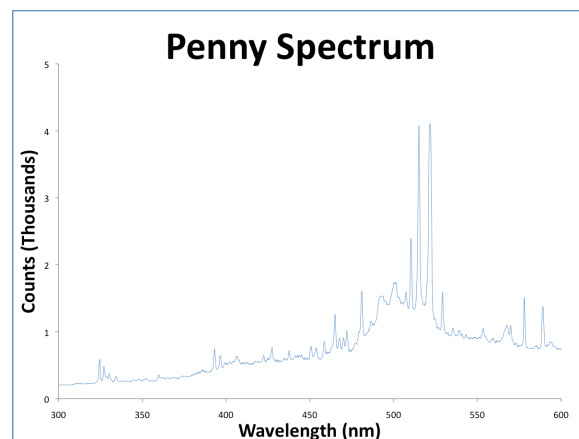
Both current US quarters and dimes have pure copper cores sandwiched between outer layers composed of 75% copper and 25% nickel (US Mint). Since our samples were taken at the surface level of the coin, it is reasonable to assume that our sample composition was 75/25% copper and nickel.



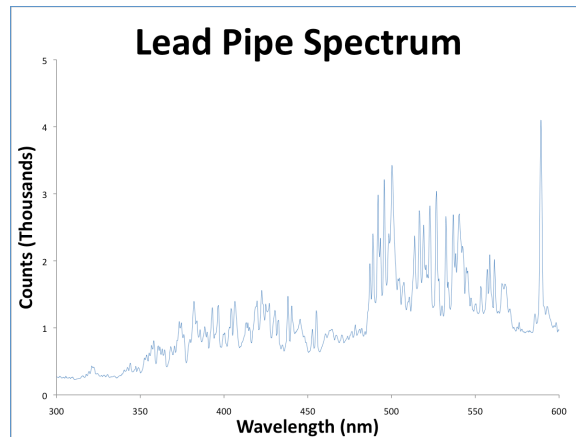
Current US nickels are not layered like the quarters and dimes, but are rather composed of a homogeneous alloy of 75% copper and 25% nickel. This should yield an identical composition in our sample to the quarter and dime spectra.



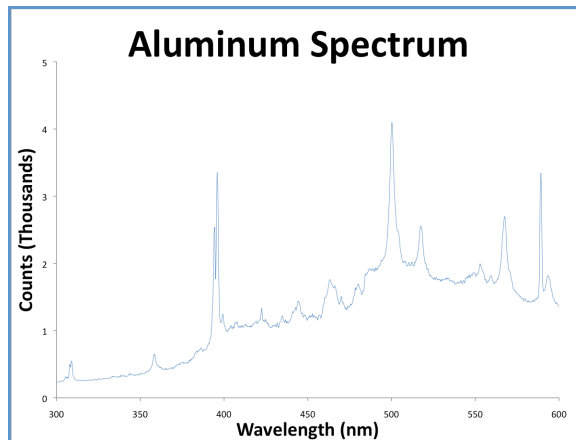
A current US penny is composed of an almost pure zinc core with a pure copper outer layer. Therefore our spectrum collected from a penny should be the spectrum for pure copper.



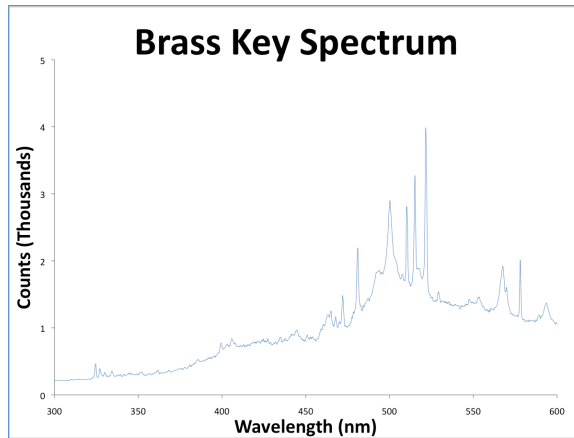
Further samples were taken of various metallic items including: a lead pipe, a brass key, and an aluminum optical apparatus. The lead pipe spectrum collected was from a pipe coated with paint, and had a large quantity of peaks as seen below.



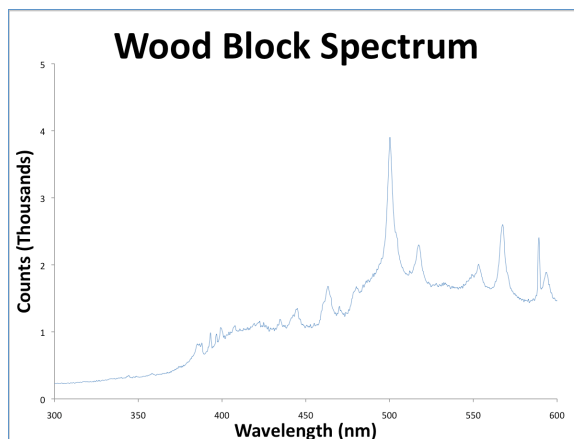
The aluminum sample was likely close to pure aluminum and had some extremely distinct peaks unique from the atmospheric spectrum.



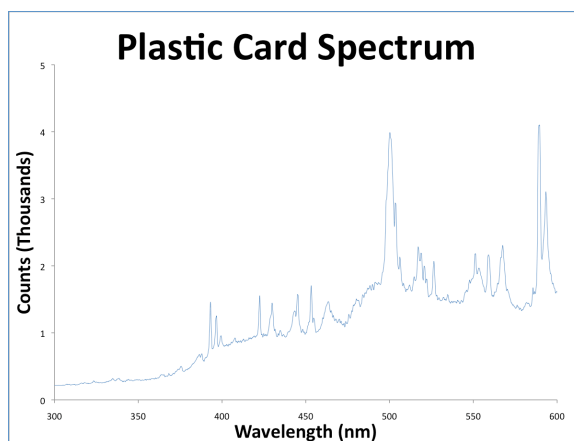
The brass key was of an unknown composition but exhibited distinct peaks that corresponded to the previously analyzed metallic samples.



Lastly, several non-metallic samples were taken including a sample from a block of wood and from the back of a plastic polymer card. The wood block spectrum is shown below.

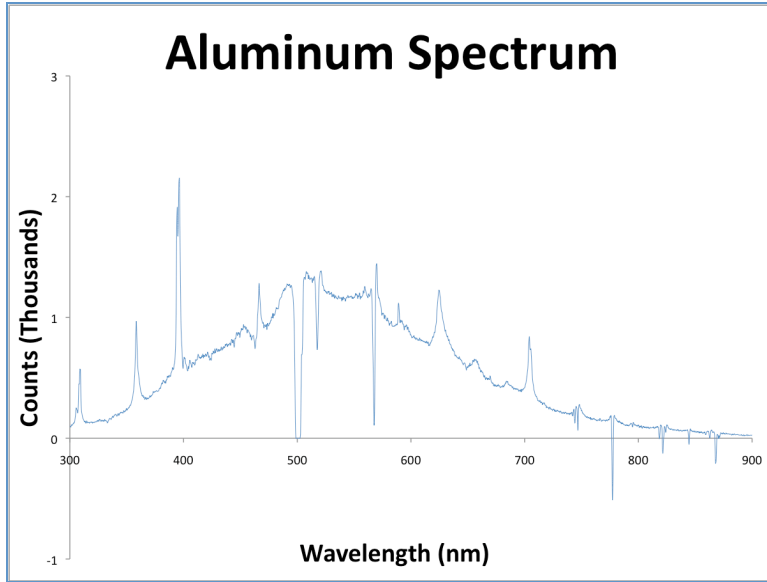


The plastic card spectrum exhibited a large quantity of distinct peaks in the lower wavelength range that were not found in the other spectra.

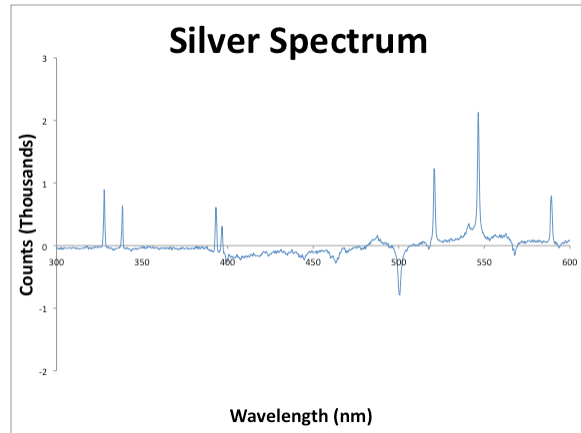
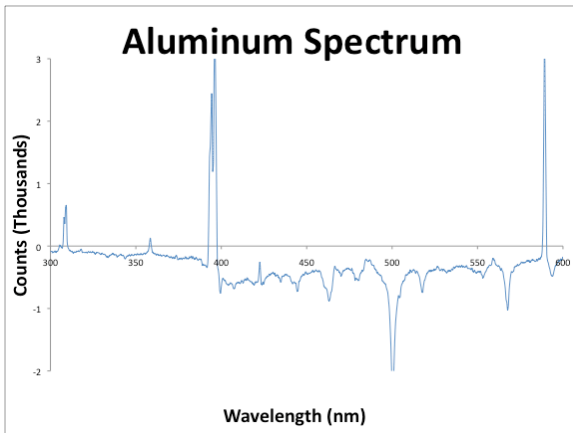


By sampling a given spectrum and recording it as a background spectrum in the spectrometer software, when a new sample is taken, the spectrometer software can automatically subtract out

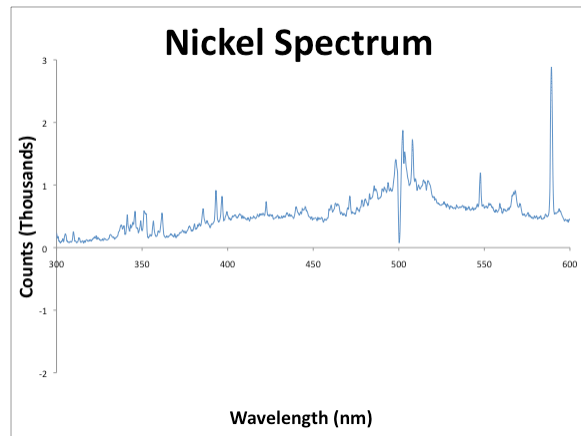
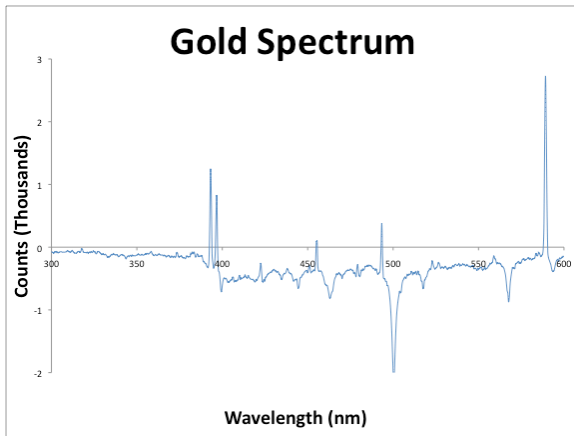
the sampled background. This technique was used on a collected aluminum sample, resulting in the spectrum below. The distinct valleys correspond to the major peaks in the atmospheric spectrum, which were subtracted out at a higher intensity than they appeared in the aluminum sample. Though the difference in relative intensities is a problem in this technique, the surviving peaks are clearly distinct to the aluminum spectrum.



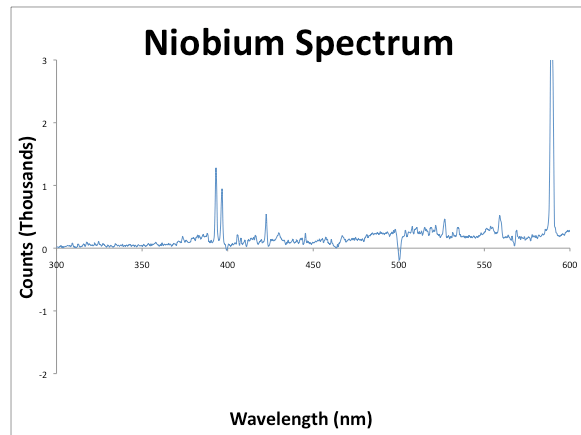
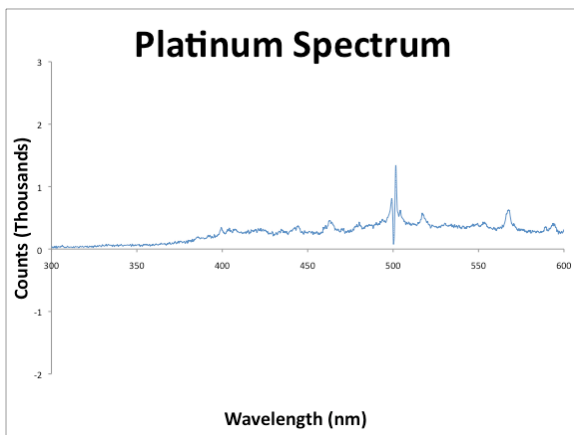
Using this technique and some pure metallic wire samples, the following spectra were collected. The background subtraction worked better with the wires because the intensities were comparable, thus providing more complete subtraction of the atmospheric portion of the background. Each sample exhibited distinct primary peaks that could be used for elemental identification in an unknown mixture.



The major peak in aluminum precisely aligns with the formerly collected aluminum spectrum.



Similarities in the nickel spectrum to the coin samples are easy to see.



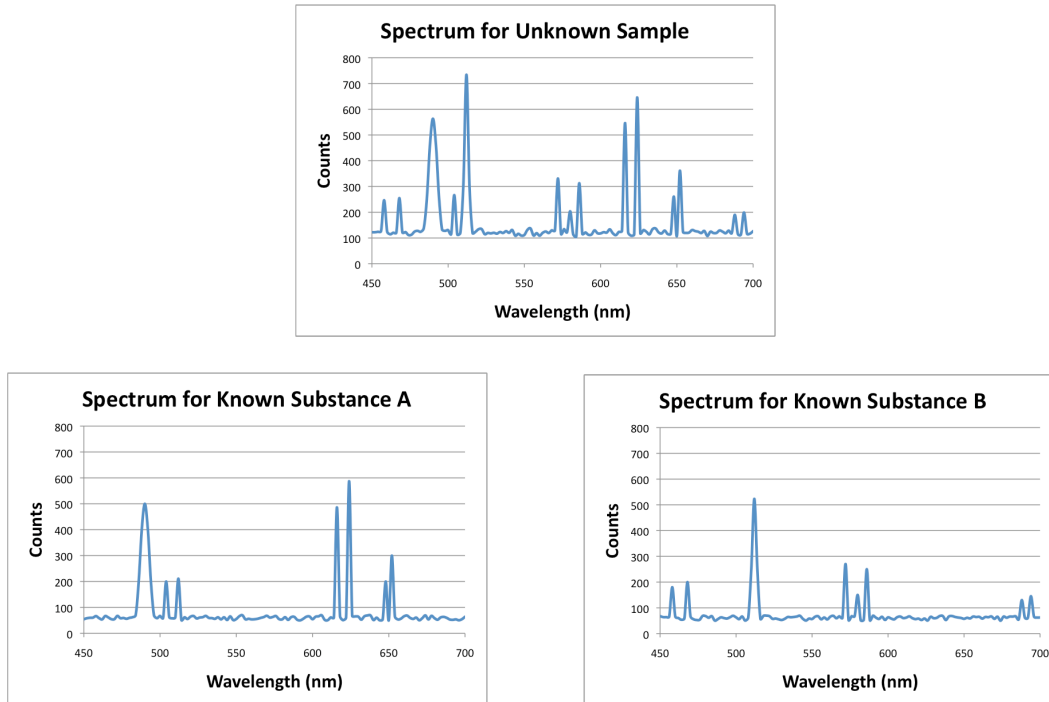
Applications: Spectroscopy of Solids

The first and most common application of a LIBS system is in the identification and matching of unknown solid samples using their collected plasma spectra. Since each individual element of the periodic table contains a unique set of excited electron energy levels, each element will emit a different spectrum of wavelengths of light when de-exciting from the plasma state. This spectrum will essentially provide us with a characteristic fingerprint for every element of the periodic table, with distinct peaks and valleys at particular wavelengths, or energies, of photons emitted. If a sample contains more than one pure element or is composed of a compound molecule, the spectra will be a superposition of each individual elemental spectrum.

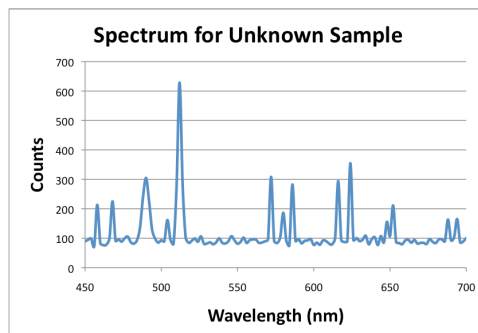
To make use of this technique, a large quantity and variety of elemental spectra would first have to be collected. The distinct wavelength locations of peaks and valleys in each spectrum would be recorded in a database for comparison to spectrums from samples of unknown composition.

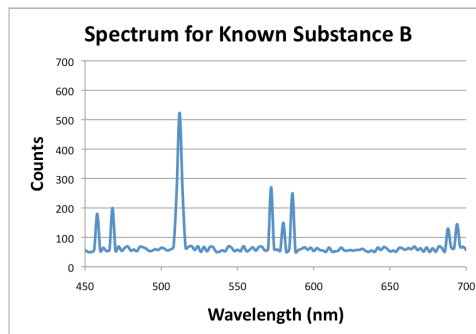
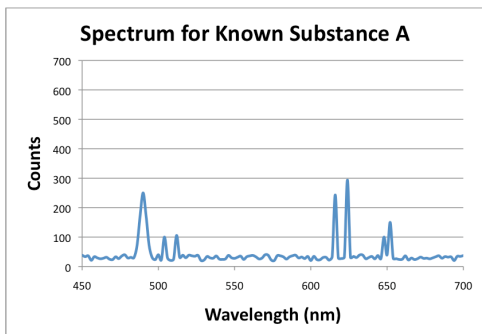
In a highly simplified hypothetical example of this technique, the unknown sample is put in the LIBS setup to collect the spectrum emitted by the plasma. The spectrum for the unknown sample is then studied to carefully identify the wavelengths of the peaks and valleys. Using the collected library of known elemental peaks and valleys, possible elemental spectrums could be matched to the unknown in order to account for all the present peaks and valleys.

This is illustrated below in the comparison between the unknown sample and known substances A and B. Though idealized, in practice the same system could be used to “reverse engineer” an unknown spectrum back to its elemental components, as the unknown spectrum is simply a superposition of each of the elemental spectra.



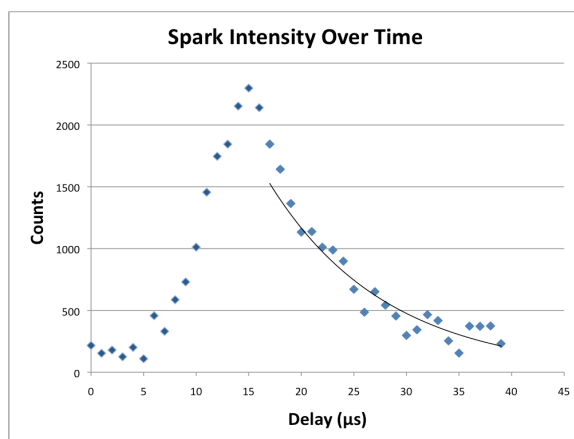
Additionally, a LIBS system with a low relative noise and high enough sensitivity could be used to not only find the elemental composition of an unknown material, but also the relative abundance of each element in the sample. The intensities of each peak in a spectrum are proportional to the quantity of the corresponding excited energy levels in the sample. Therefore, by comparing the intensities of the primary peaks present from each elemental spectrum, the relative composition of an unknown material could also be calculated.





A further, theoretical application of the LIBS setup is to measure the lifetimes of individual excited electron states in the plasma formed from different materials. During the formation of the plasma, the excitation of electrons does not happen concurrently with the de-excitation that forms the observed spark. Rather, the energy from the incident photons and electric field excites a maximum quantity of electrons to their excited states. The electrons stay in these excited states for a period of time but soon begin to fall out of their excited states, returning to ground state by emitting a photon. The electrons stay in the excited state for an average lifetime, resulting in an exponential decay similar to the decay of a radioactive source. Since the de-exciting electrons emit photons creating the spark, the intensity of the spark over time is proportional to the decay rate of the excited electrons. If multiple intensity snapshots of a single peak within a plasma spark could be taken over time, an exponentially decaying equation could be fit to the tail of the spark decay, yielding a decay constant and lifetime for the individual excited energy state.

Experimentally, these intensity snapshots of the spark could be obtained by delaying the Q-switch trigger pulse in small increments and recording the counts at a specific wavelength over multiply trials. In this experiment, these small delays are created using the pico-second delay generator, which is connected between the spectrometer and the laser control on the Q-switch input line. Though this LIBS system was found to lack the timing precision necessary to take multiple measurements over the duration of the plasma lifetime, if the system could achieve such precision the collected data might look something like the hypothetical plot below.



The tail of the exponential decay has been fit to a line of the form:

$$Counts = Ae^{-\frac{1}{\tau}t}$$

The coefficient A simply scales the line to fit the maximum intensity, but the fit would also yield τ , the lifetime of the excited state.

Conclusions

Through this research we successfully created a functional LIBS setup, which was verified to be working correctly using known samples. Though we were unable to fully utilize the setup for determining the composition of unknown, the theory was seen to be functional. Especially the data taken of the pure wire samples at the end of the research clearly showed distinct emission lines in the plasma deionization for each element.

Poster

This research was submitted to the College of Science and Math Student Research Conference as the poster shown below:

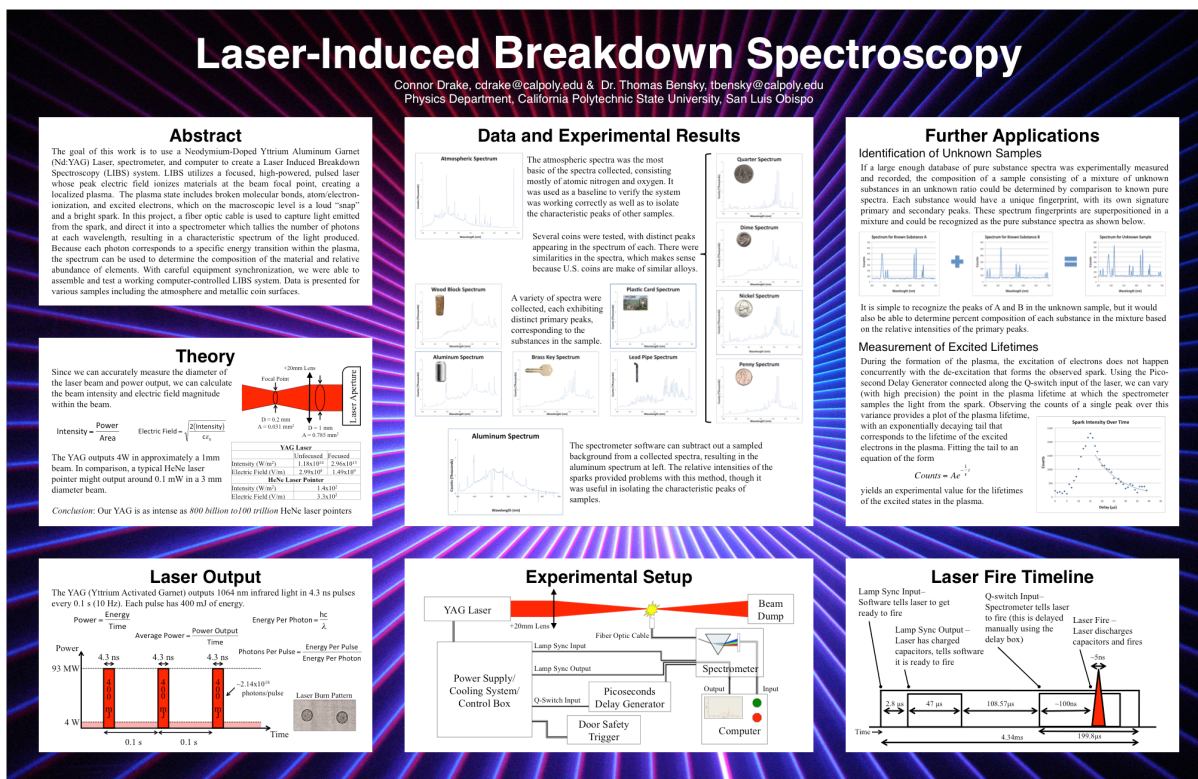


Figure 11: Research poster for SCM Research Conference

References

Knopp, R., Scherbaum, F.J., and Kim J.I., 1996, "Laser induced breakdown spectroscopy of metal ions in aqueous solutions", *Anal. Chem.*, **355**, 16-20.

Radziemski, L.J., Loree, T.R., Cremers, D.A., and Hoffman, N.M., 1983, "Time-resolved, laser-induced breakdown spectroscopy of aerosols." *Anal. Chem.*, **55**, 1246-1252.

Singh, J.P., Zhang, H., Yueh, F.Y. and Carney, K.P., 1996, "Investigation of the effects of atmospheric conditions on the quantification of metal hydrides using laser induced breakdown spectroscopy", *Appl. Spectrosc.*, **50**, 764-773.

Yueh, F., Singh, J.P., and Zhang, H., 2000, "Laser-induced breakdown spectroscopy, elemental analysis.", *Encyclopedia of Anal. Chem.*, 2066-2087.